Patterns, Volume *2*

Supplemental information

An intra-host SARS-CoV-2 dynamics model to assess testing and quarantine strategies for incoming travelers, contact management, and de-isolation

Wiep van der Toorn, Djin-Ye Oh, Daniel Bourquain, Janine Michel, Eva Krause, Andreas Nitsche, Max von Kleist, and on behalf of the Working Group on SARS-CoV-2 Diagnostics at RKI

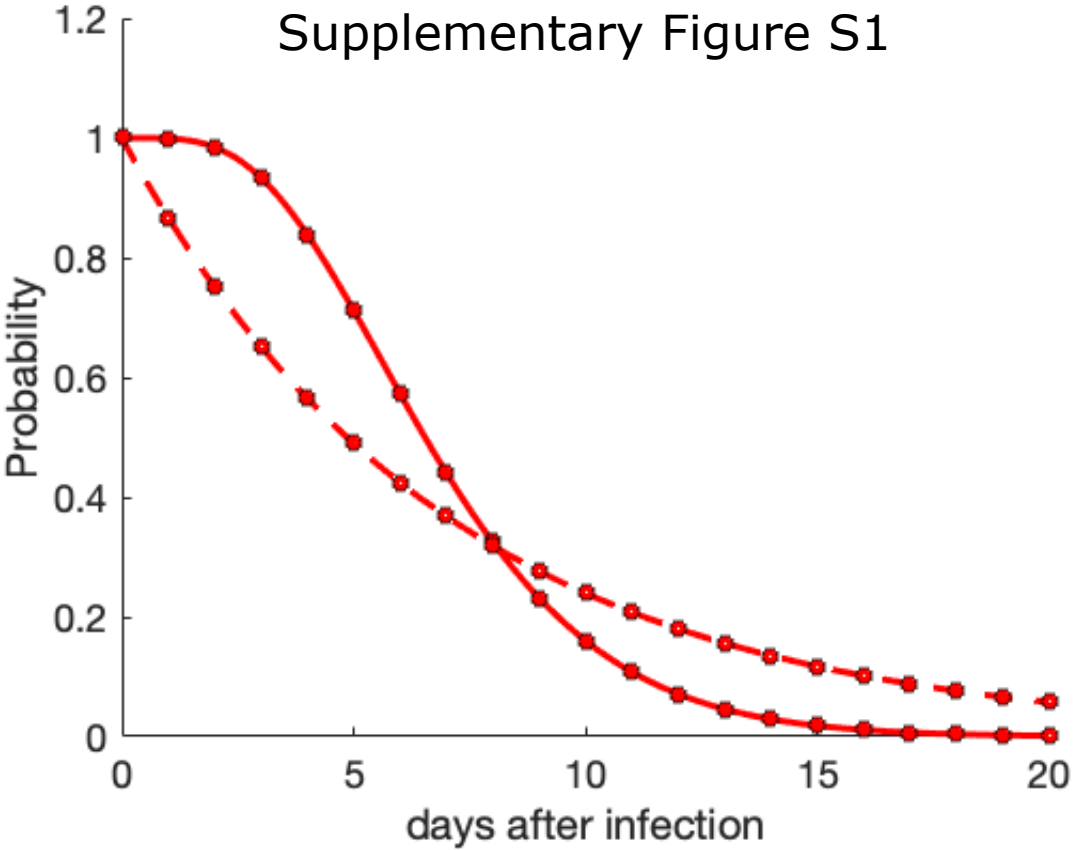

Supplementary Figure S1: **Illustration of how introducing compartments can alter the shape of the residence time without affecting its mean**. Example with τ=5 days. Dashed line: one sub-compartment with rate r=1/τ. Solid line: n=5 five sub-compartments with rates r_i=n/τ.

Supplementary Figure S2

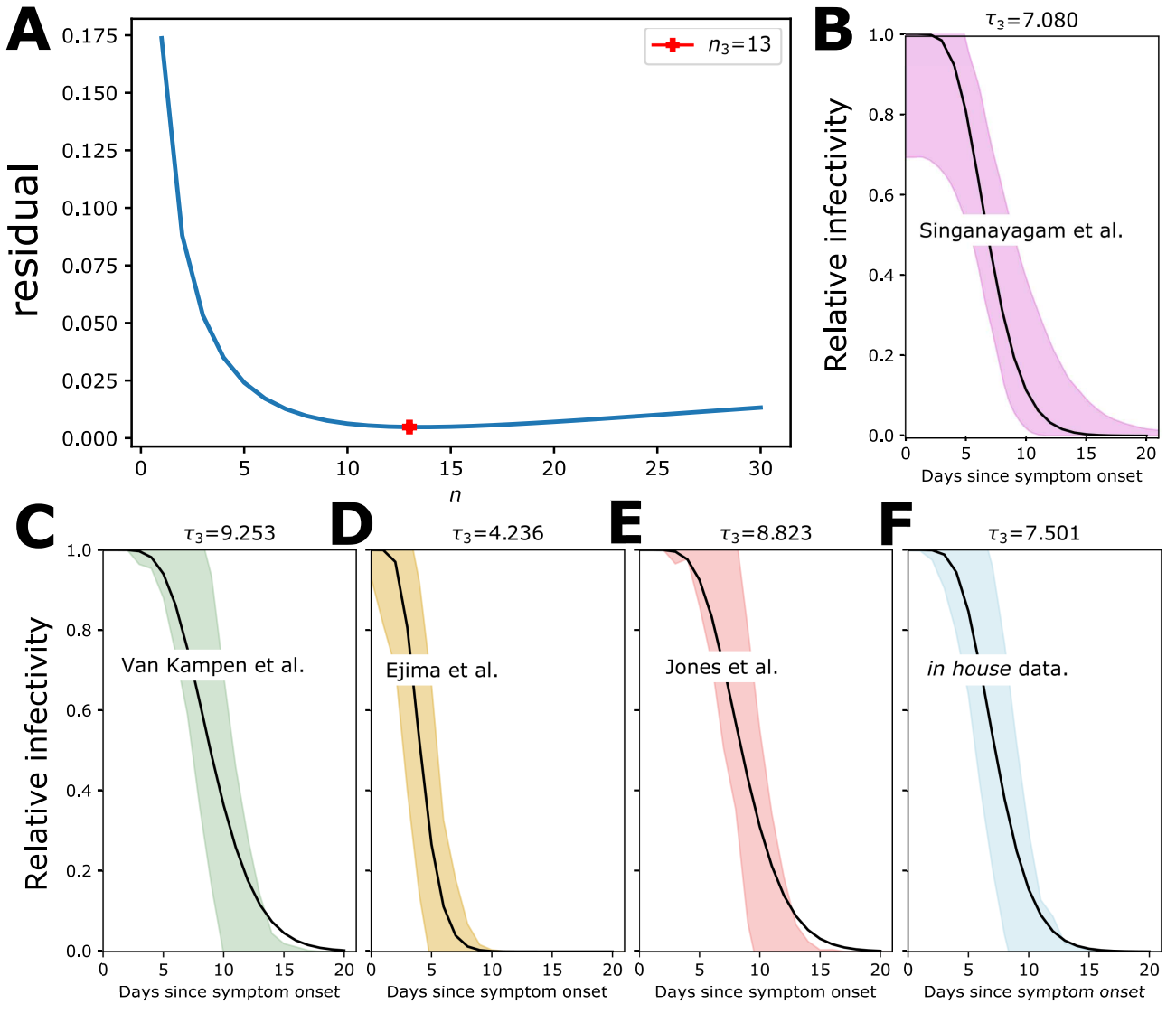

Supplementary Figure S2: **Parameter estimation for the infectious (& symptomatic) phase, j = 3.** A: Hyperparameter search for the number of compartments n_3 in the infectious (& symptomatic) phase. B-F: Fits to the individual studies.

Supplemental Experimental Procedures

SN.1 Analysis of infectivity profiles

Below we describe the mathematical analysis of *in house* data. More precisely, how to transform raw viral measurements (PCR cycle time (Ct) values) and associated measurements of culture positivity in order to arrive at infectivity profiles after symptom onset. The deduced infectivity profiles are used alongside published data to estimate parameters of phase 3 (number of sub-compartments and mean residence time in the phase where an individual has symptoms and may disseminate infectious virus particles).

We will first pursue a mechanistic modelling which allows to put viral kinetics, as well as immune-related virus neutralisation into context. We fit this model to *in house* data that reports viral kinetics, culture-positivity and time since symptom onset. Using the mechanistic modelling, we are then enabled to deduce an attack rate curve z_t from viral load profiles, for studies that do not report infectivity explicitly (inputing some parameters learned from the *in house* data).

The mechanistic model is then used to derive the attack rate curve z_t for each considered data set where this curve is not explicitly stated and used for deriving default parameters for our Markov model (Fig. 1A, main manuscript).

SN.1.1 Mechanistic modelling

We will model the attack rate as a function of the viral kinetics in the potential transmitter, as well as virus neutralisation within the host. Under the reasonable assumption of statistical independence the probability of infection (attack rate) can be written as

$$z_t \quad = \quad 1 - c_1^{\left(V_{eI}(t)\right)} \tag{SN.1}$$

where $0 << c_1 < 1$ is the probability of non-infection after exposure to a single infectious virus. The exposure with *infectious* virus $V_{eI}(t)$ can be thought of as a Bernulli process (compare below) and hence is a binomially distributed random number. The expected exposure to *infectious* virus is then $\mathbb{E}\big(V_{eI}(t)\big) = F_I(t) \cdot V_e(t)$, which we will use henceforth.

SN.1.1.1 Virus exposure $V_e(t)$

The virus exposure $V_e(t)$ can be assumed to be a function of the viral load $VL(t)$ in the respiratory tract of an infected individual. Viral kinetics have been elaborated in several studies, e.g. [1, 2]. Typically, the viral titers increase exponentially, reaching a set point at about symptom onset and decrease exponentially thereafter. Viral exposure $V_e(t)$ emanating from an infected individual can be thought of as being a fraction of the viral load in the respiratory tract. This can be modelled, akin to [3], as a Bernulli Process, hence,

$$V_e(t) \sim \mathcal{B}(p, VL(t)) \tag{SN.2}$$

where $\mathcal{B}$ is the binomial distribution and p the success probability (fraction of virus load that is exposed to the recipient). The binomial distribution has expectation value $\mathbb{E}\big(V_e(t)\big) = p \cdot VL(t)$, which we will use henceforth.

SN.1.1.2 Fraction of infectious virus $F_I(t)$

It has been shown in several studies [4–6] that the infectiousness of virus from patient samples decreases as a function of the time since symptom onset. This is generally believed to be a result of neutralization

by antibodies [7,8]. Notably, neutralisation in the upper respiratory tract may occur before it is detectable in the blood plasma. Let us assume that the immune system response $IR(t)$ increases exponentially after infection. Then, the fraction of infectious virus $F_I(t)$ can be modelled by Emax kinetics [9]

$$F_I(t) = \frac{1}{1 + \widehat{IR}(t)} \tag{SN.3}$$

where $\widehat{IR}(t)$ is proportional to the immune response. An interpretation would be $\widehat{IR}(t) = Ab(t)/\mathrm{IC}_{50}$ (concentration of neutralising antibodies divided by their fifty percent inhibitory concentration).

SN.1.2 The shape of the attack rate curve

In case of an exponential increase of the immune response, $\widehat{IR}(t_e) = \widehat{IR}(t_{0,e}) \cdot e^{\left(t_e \cdot c_3\right)}$, where $t_{0,e}$ is the time *of* exposure and t_e is the time *after* exposure and hence $t_e = t + \tau_{\mathrm{inc}}$.

$$\begin{aligned} z_t &= 1 - c_1^{\left(V_{eI}(t)\right)} = 1 - c_1^{p \cdot VL(t) \cdot F_I(t)} && \text{(SN.4)} \\ z_t &= 1 - c_1^{p\left[\frac{VL(t)}{1+\left(\widehat{IR}(t_{0,e}) \cdot e^{((t+\tau_{\mathrm{inc}}) \cdot c_3)}\right)}\right]} && \text{(SN.5)} \\ &= 1 - c_1^{p\left[\frac{VL(t)}{1+g(c_3) \cdot e^{(t \cdot c_3)}}\right]} && \text{(SN.6)} \end{aligned}$$

where $g(c_3) = \left(\widehat{IR}(t_0^e)\right) \cdot e^{(\tau_{\mathrm{inc}} \cdot c_3)}$.

SN.1.3 Estimation of infectivity profiles from *in house* data

SN.1.3.1 Viral dynamics

We first estimate the viral decay kinetics based on the Ct values. The data is depicted below in Fig. SN.1, left. We first use a sliding window technique to extract the average slope of the Ct values (blue line) to which we then fit a linear equation in the temporal range $t \in [0 \;\; 20]$ by minimizing the least squares deviation.

$$\begin{aligned} y_t &= m \cdot t + y_0 && \text{(SN.7)} \\ &\text{with} \\ Ct(t) &= y_t + \varepsilon && \text{(SN.8)} \end{aligned}$$

with optimal parameter $m^* = 0.43$. We assumed an additive error (which justified the least squares regression) and estimated $\varepsilon \sim \mathcal{N}\left(0, \sigma^2\right)$, where $\sigma^2 = 4.44$. The resulting simulated Ct values are depicted in Fig. SN.1, middle.

As illustrated by [10], Ct values are linearly correlated with $\log_{10}$ viral loads (genome equivalents/μL), i.e.:

$$\begin{aligned} -c \cdot \log_{10}(VL(t)) + k &= Ct(t) && \text{(SN.9)} \\ \log_{10}(VL(t)) &= \frac{1}{c} Ct(t) + \frac{k}{c} && \text{(SN.10)} \end{aligned}$$

For the *in house* PCR assay we have $c = 3.35$ for the Charité E protein primers used in our study and therefore $\frac{1}{c}$ is very close to the idealised value of $\frac{1}{\log_2(10)} \approx 0.3$.

Finally, the slope parameter for the viral loads (combining the Ct(t) slope and the linear regression parameter) is $\tilde{m} = m/c = 0.133$ (day^{-1}). Similarly, the variance gets scaled to $\tilde{\sigma}^2 = 4.44/c = 1.32$, now being an exponential error, i.e. $\epsilon \sim \mathcal{N}\left(0, 1.32\right)$. The actual viral loads depend on the intercept, which in turn depends on the extraction of viral samples, as well as on the configuration of the assay in the respective lab. We therefore chose to set the average viral loads to published values [4], i.e. $\mathbb{E}\left(VL(t_0)\right) \approx 6 \cdot 10^7$ (copies/swab)$\Rightarrow \tilde{y}_0 = 7.77$.

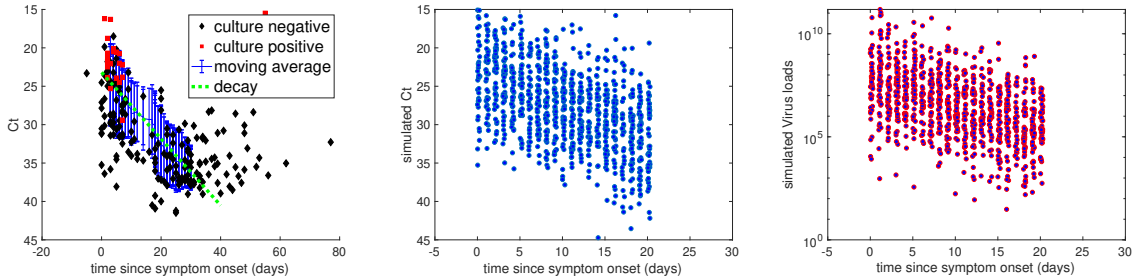

Fig SN.1. Own data and data fitting. Left: Ct values from Sars-CoV2 infected individuals after symptom onset. Black dots denote culture negative- and red dots culture positive samples. The solid blue line with error bar denotes the sliding average and the dashed green line is a fitted increase in Ct with slope 0.4 (day^{-1}) and intercept 24. **Middle:** Simulated Ct values using eq. (SN.7). **Right:** Simulated genome equivalents/mL.

SN.1.3.2 Attack rate

We use the equation for the attack rate (compare eq.(SN.6)).

$$z_t \quad = \quad 1 - c_1{}^{p\left[\frac{VL(t)}{1+g(c_3)\cdot e^{(t\cdot c_3)}}\right]} \tag{SN.11}$$

where $g(c_3) = \widehat{IR}(t_0^e) \cdot e^{(\tau_{\text{inc}} \cdot c_3)}$. We will set $\widehat{IR}(t_0^e) = 0.01$.

This leaves us with three free parameters: $10^{-6} < p < 0.01$ and $0.01 < c_3 < 3$ and $0.99 \leq c_1 < 0.9999$.

We now minimize

$$\{p^*, c_3^*, c_1^*\} = \text{argmin}\Big(\big(\psi \cdot w - z_t\big)^2\Big), \tag{SN.12}$$

where $\psi \in [0, 1]$ denotes the data (culture negative or culture positive). We assessed different values for the hyperparameter (weight) w, see below in Fig. SN.2. The weighing parameter w is intended to put more importance on the culture positive samples, as there may be false negative cultures due to transportation and storage of samples. This also puts more emphasis on increasing the sensitivity of the method (less false negative predictions), as it increases the methods' safety margin. After hyperparameter scan we selected $w = 3$. Predicted infectivity profiles and diagnostic plots are depicted in Fig. SN.2.

SN.1.3.3 Summary and optimal parameters.

Using the methods described above, we get the following optimal parameters: $p = 0.01$, $c_3 = 0.741$, $c_1 = 0.99$. Using these values the model has a sensitivity of $sens = 96\%$ and a specificity of $spec = 0.57\%$.

Sensitivity was computed as:

$$sens. = P(pred.\ positive|culture\ positive) = \frac{A(t)|\text{culture pos.}}{\#\text{culture pos.}} \tag{SN.13}$$

Specificity was computed using

$$spec. = P(pred.\ negative|culture\ negative) = 1 - \frac{A(t)|\text{culture neg.}}{\#\text{culture neg.}} \tag{SN.14}$$

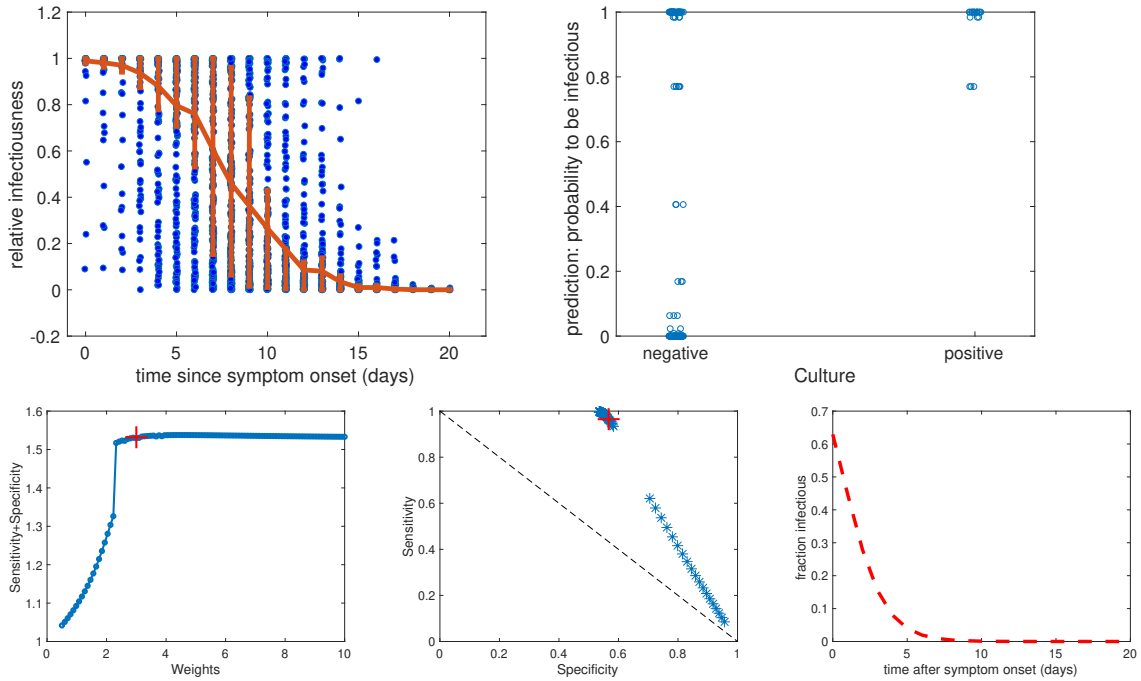

Fig SN.2. Fitting to *in house* data. Upper Left: Predicted relative infectivity based on sampled viral loads (compare Fig. SN.1 and estimated parameters, eq. (SN.12). Blue dots: Sampled infectivity values, red line and error bars: mean infectivity and inter-quartile range. **Upper Right:** Predicted attack rate vs. positive culture. **Lower Left:** Scanning of hyper parameters (weights). Red cross: chosen weight. **LowerMiddle:** Sensitivity and specificity for different hyper parameters. **Lower Right:** Predicted fraction of infectious virus, using $\frac{1}{1+g(c_3)\cdot e^{(t\cdot c_3)}}$.

References

1. Ejima K, Kim KS, Ito Y, Iwanami S, Ohashi H, Watashi YKA, et al. Inferring Timing of Infection Using Within-host SARS-CoV-2 Infection Dynamics Model: Are "Imported Case" Truly Imported. medRxiv (https://doiorg/101101/2020033020040519). 2020;.

2. Jones TC, Biele G, Mühlemann B, Veith T, Schwarzer R, Zuchowski M, et al. Analysis of SARS-CoV-2 viral load and infectivity from 9009 RT-PCR-positive cases in Germany. submitted. 2020;.

3. Duwal S, Sunkara V, von Kleist M. Multiscale Systems-Pharmacology Pipeline to Assess the Prophylactic Efficacy of NRTIs Against HIV-1. CPT Pharmacometrics Syst Pharmacol. 2016;5(7):377–87. doi:10.1002/psp4.12095.

4. Wölfel R, Corman VM, Guggemos W, Seilmaier M, Zange S, Müller MA, et al. Virological assessment of hospitalized patients with COVID-2019. Nature. 2020;581(7809):465–469. doi:10.1038/s41586-020-2196-x.

5. Singanayagam A, Patel M, Charlett A, Lopez Bernal J, Saliba V, Ellis J, et al. Duration of infectiousness and correlation with RT-PCR cycle threshold values in cases of COVID-19, England, January to May 2020. Euro Surveill. 2020;25(32). doi:10.2807/1560-7917.ES.2020.25.32.2001483.

6. van Kampen JJA, van de Vijver DAMC, Fraaij PLA, Haagmans BL, Lamers MM, Okba N, et al. Shedding of infectious virus in hospitalized patients with coronavirus disease-2019 (COVID-19): duration and key determinants. MedRxiv (https://doiorg/101101/2020060820125310). 2020;.

7. Meyer B, Reimerink J, Torriani G, Brouwer F, Godeke GJ, Yerly S, et al. Validation and clinical evaluation of a SARS-CoV-2 surrogate virus neutralisation test (sVNT). Emerg Microbes Infect. 2020;9(1):2394–2403. doi:10.1080/22221751.2020.1835448.

8. Liu L, To KKW, Chan KH, Wong YC, Zhou R, Kwan KY, et al. High neutralizing antibody titer in intensive care unit patients with COVID-19. Emerg Microbes Infect. 2020;9(1):1664–1670. doi:10.1080/22221751.2020.1791738.

9. Shen L, Peterson S, Sedaghat AR, McMahon MA, Callender M, Zhang H, et al. Dose-response curve slope sets class-specific limits on inhibitory potential of anti-HIV drugs. Nat Med. 2008;14(7):762–6. doi:10.1038/nm1777.

10. Vogels CBF, Brito AF, Wyllie AL, Fauver JR, Ott IM, Kalinich CC, et al. Analytical sensitivity and efficiency comparisons of SARS-CoV-2 RT-qPCR primer-probe sets. Nat Microbiol. 2020;5(10):1299–1305. doi:10.1038/s41564-020-0761-6.